GSA DATA REPOSITORY 2015261

Supplementary information for

The geological CO_2 degassing history of a long-lived caldera

Giovanni Chiodini[1], L. Pappalardo[2], A. Aiuppa[3], and S. Caliro[2]
[1]INGV, Sezione di Bologna, via Creti 12, 40128 Bologna, Italy
[2]INGV, Sezione di Napoli, via Diocleziano 328, 80124 Napoli, Italy
[3]Dipartimento DiSTeM, Università di Palermo, Via Archirafi 36, 90123 Palermo, Italy
[4]INGV, Sezione di Palermo, via La Malfa 153, 90146 Palermo, Italy

MATERIALS AND METHODS

The data obtained in this research refer to rock samples from three deep geothermal boreholes drilled by Agip in the caldera area (Mofete5, Licola1 and S. Vito1 wells) as well as plutonic syenitic clasts included in the Breccia Museo deposit.

Stable isotope compositions of carbon and oxygen on hydrothermal calcite and its concentration have been determined at Istituto Nazionale di Geofisica e Vulcanologia in Naples on powder samples by using a Spectrometer Finnigan Mat Delta plus. The accuracy of the measurements is ± 0.15 ‰ for $d^{13} C_{CO2}$, ± 0.1 ‰ for $d^{18} O$, and ± 10% for calcite concentration ($C_{calcite}$) (Table DR1). The CF data set was completed with previous published oxygen and carbon calcite compositions of Mofete 1 well (M1-1302 and M1-1500, Caprarelli et al., 1997) and of CFDDP (CFDDP-443 and CFDDP-506, Mormone et al., 2015) (Table DR1).

Polished thin sections of rock samples were analyzed by: (i) polarized light microscopy for a preliminary identification of the mineralogical assemblage, (Table DR1) and (ii) by electron microprobe (EMPA) for measurements of major element compositions of hydrothermal minerals, performed at Istituto Nazionale di Geofisica e Vulcanologia in Rome with a JEOL-JXA-8200 electron microprobe (WD/ED combined micro analyzer) using 15 kV voltage, a 10 mm beam spot and 10 nA beam current. The analytical uncertainty was about 1% for most elements. Results are reported in Table DR2.

STRATIGRAPHIC DESCRIPTION AND PETROGRAPHY OF STUDIED ROCKS

Samples were collected at different depths of three geothermal boreholes drilled in the proximity of the western border (Mofete5 and Licola1 wells) as well as in the central sector (S. Vito1 well) of the caldera, Figure DR1 (Agip, 1987, Rosi and Sbrana, 1987). In the western border of the caldera (Mofete 5 and Licola 1 wells) the cored stratigraphic succession is represented by pyroclastic rocks of post-caldera period, that buried a sequence of sedimentary submarine rocks inter-bedded with tuffs, tuffites and lava bodies. On the contrary, S. Vito 1 well, in the central sector of the caldera, has encountered prevalently the volcanic tuffs filling the calderic depression. Particularly, under a 500 meter thick pyroclastic succession of post-caldera age, two main volcanic tuff formations have been penetrated: a yellow tuff between 500 and 1000 m of depth and a gray tuff between 1000 and 2000 m of depth, probably emplaced during the two large-scale eruptions of the Neapolitan Yellow Tuff (14 ka) and of the Campanian Ignimbrite (40 ka), respectively.

The stratigraphy and the temperature profiles of the boreholes are shown in Figure DR1 with the sample locations. The sample name represents the specific well followed by the depth at which

the sample was taken (i.e. M5 1284, Mofete 5 well, 1284 m of depth) while Breccia Museo ejecta are from two sites: Acquamorta at Monte di Procida, (samples: BM S-5-1, S-5-2,) and Punta della Lingua on Procida Island (samples BM S-1, S-2, S-3, S-4). Moreover, the distributions of mineral phases as a fuction of the temperature measured in the wells is reported in Table DR3.

Mofete 5 well. : The sample M5 1284 is a porphyritic lava with phenocrysts of feldspar and magnetite included in microcrystalline groundmass, secondary minerals of calcite, sericite and chlorite are widespread in the whole-rocks. The sample M5 1749 is a volcanic tuff, constituted by phenocrysts of feldspar and subordinately apatite dispersed in matrix glass, secondary minerals of calcite, sericite and chlorite are present in the matrix. The sample M5 2603 is an intrusive syenite constituted by primary minerals of feldspars, and secondary of calcite, quartz, siderite, epidote, zircon and scapolite. The samples M5 2488 and M5 2696 belong to a deep volcanic tuffites characterized by fine-grained cineritic matrix in which are widespread polygenic lithic clasts and scoriae. Phenocrysts are represented by euhedral and subeuhedral alkali feldspar, biotite, magnetite, and clinopyroxene. Calcite is also present as well as epidote, pyrite, quartz, siderite, scapolite, sphene and amphibole.

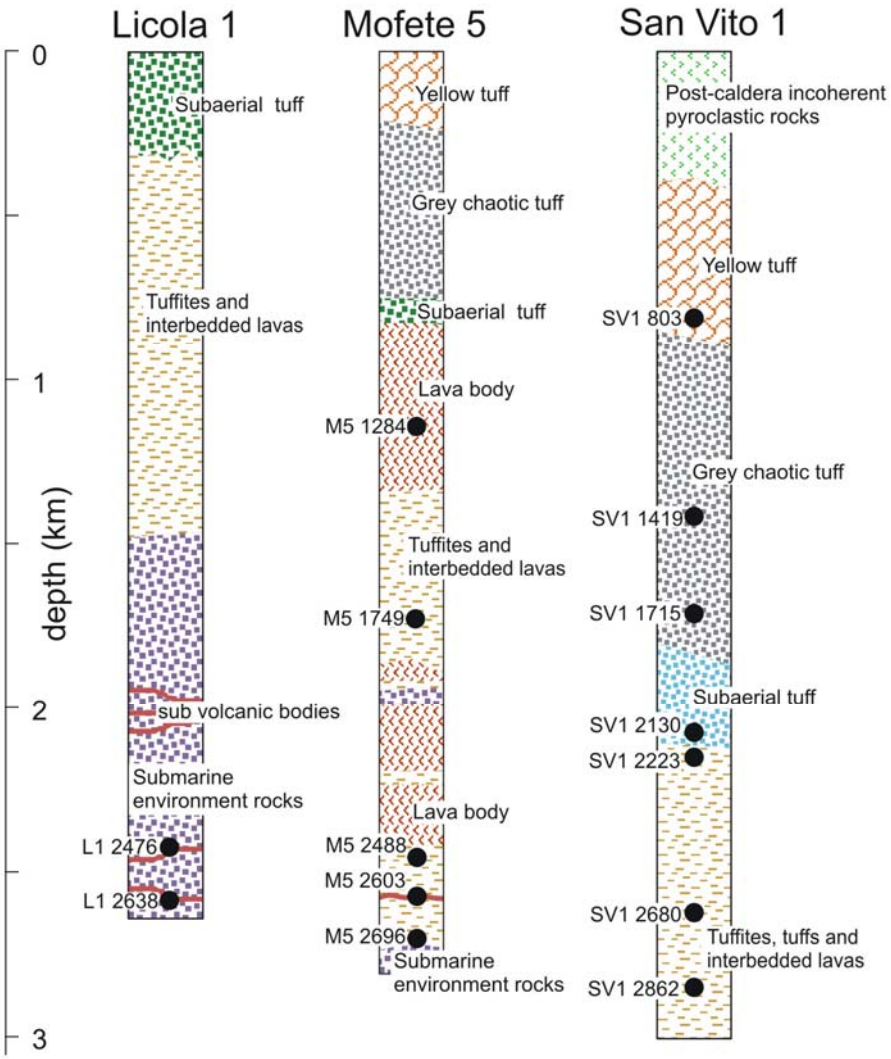

Figure DR1 – Lithostratigraphic sections of the studied geothermal boreholes.

Licola1 well : The samples L1 2476, is a porphyritic lava with phenocrysts of plagioclase and alkali feldspar, with advanced sericite-type alteration process, albite, calcite and pyrite are also present. The sample L1 2638 is a deep lava body constituted by phenocrysts of feldspars, biotite, magnetite and apatite and secondary minerals of albite, calcite, chlorite, sericite, perovskite, fluorite, zircon.

S. Vito 1: Sample SV1 803 belongs to the Neapolitan Yellow Tuff formation and consists phenocrysts of k-feldspar, magnetite and cpx. Secondary minerals include sodalite, sericite, calcite. The samples SV1 1419 and SV1 1715 are part of the Campanian Gray tuff. They are constituted by euedral phenocrysts of sanidine, plagioclase, clinopyroxene, magnetite, biotite and apatite distributed in an abundant altered matrix-glass. Secondary minerals include sericite, calcite, chlorite, albite and zeolite. Below the Campanian gray tuff, pre-calderic rocks are formed by the alternation of volcanic tuffs, lavas and tuffites. The sample SV1 2130 is constituted by a gray tuff formed predominantly by phenocrysts of plagioclase included in an altered matrix glass with abundant secondary minerals of calcite, chlorite, pyrite and quartz; while the sample SV1 2862 belongs to a deeper volcanic tuff formed by phenocrysts of plagioclase, clinopyroxene, magnetite and secondary minerals of sericite, calcite, pyrite, epidote. Reworked levels (SV1 2223 and 2680) are intercalated between the latter pre-calderic tuffs. In these deep samples the primary structure is no longer recognizable, while predominate secondary minerals of sericite, calcite, chlorite, pyrite, quartz, amphibole, epidote.

Syenitic plutonic clasts: The syenitic clasts are consitituted prevalently by subhedral to anhedral potassium feldspar (70%) and plagioclase (20%). Cancrinite (hauyna) was identified as a minor component in some samples. Mafic mineral assemblages are constituted by clinopyroxene and biotite often intergrown with chlorite. Hornblende is often present as an overgrowth over relict clinopyroxene. Accessory minerals are zircon and sphene, apatite, opaques (ilmenite), garnet, scapolite, fluorite, pistacite.

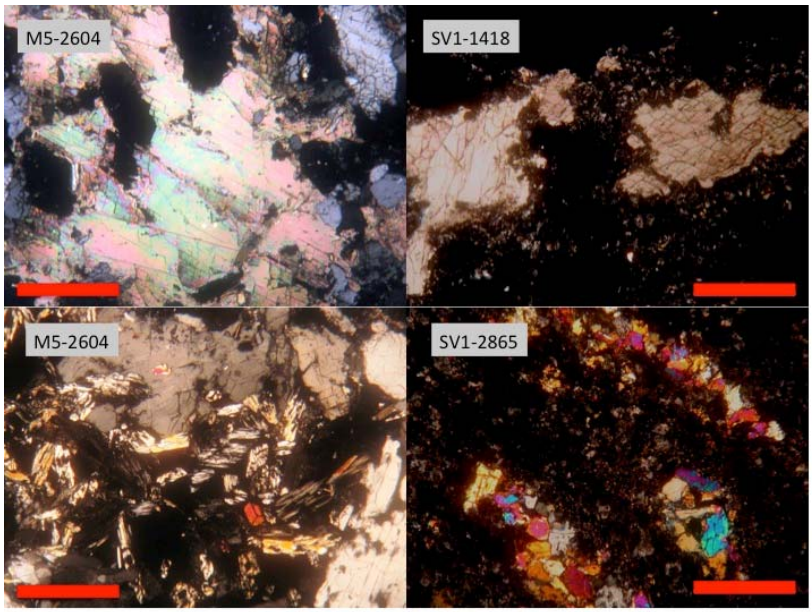

Figure DR2 A) –Examples of back-scattered electron images of polished thin sections representative of samples from studied wells. B) Examples of photomicrographs of thin sections of samples from studied wells. Scale bars represent 1000 μm. Upper images: calcite crystals, cross-polarized light; lower images: epidote crystals, cross-polarized light.

COMPUTATION OF THE AVERAGE CALCITE CONCENTRATION

The $C_{calcite}$ dataset of core samples (i.e. excluding the Breccia Museo sample) define, in a log-probability plot (Supplementary Figure 3), a curve with an inflection point that we interpret as due to the presence of two overlapping log-normal populations. Applying the graphic method of Sinclair (1974), the original dataset can be partitioned into two log-normal populations, with respectively high (Population A, 70%) and low (Population B, 30%) $C_{calcite}$ values.

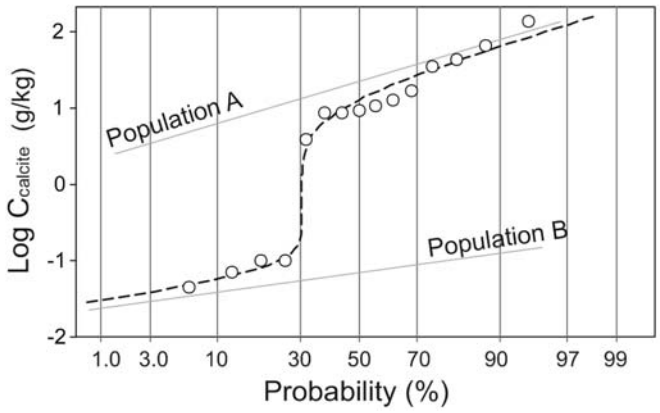

Figure DR3 – Probability plot of $C_{calcite}$ and partitioning of the data in the two log-normal populations A and B.

We used a Montecarlo procedure to estimate the mean $C_{calcite}$ values, M_i (and their 90% confidence intervals), for both populations; these resulted $M_B = 0.08$ g kg^{-1} (90% c.i from 0.052 g kg^{-1} to 0.113 g kg^{-1}) for population B, and $M_A = 36.7$ g kg^{-1} (90% c.i from 18.8 g kg^{-1} to 65.1 g kg^{-1}) for population A. Considering the fractions of the two populations we estimate an average $C_{calcite}$ of 25.7 g kg^{-1} (90% confidence interval from 13.2 g kg^{-1} to 45.6 g kg^{-1})

TABLE DR1. PARAGENESIS AND CHEMICAL-ISOTOPIC COMPOSITION OF THE ANALYZED ROCKS

	lithology	**T** (°C)	**primary minerals**	**hydrothermal minerals**	C_{CaCO3} (g / Kg)	$^{13}C_{calcite}$ (d‰)	$^{18}O_{calcite}$ (d‰)
SV1 803	tuff	130	k-fld, mt, cpx	sod, ms, cc, py	8.81	-0.86	14.68
SV1 1419	tuff	260	k-fld, pl, cpx, ap, ti-mt, bt	zeol, ms, cc, ab	12.9	-2.76	14.63
SV1 1715	tuff	285	k-fld, pl, cpx, ap, ti-mt, bt	ms, cc, chl	10.9	-1.42	8.49
SV1 2130	tuff	300	k-fld	ms ,cc, chl py, qz, ab	0.045	n.d.	n.d.
SV1 2223	reworked	320	not recognizable crystals	cc, chl py, qz, amp	8.63	-3.90	18.81
SV1 2680	reworked	350	not recognizable crystals	ms, cc, py, ep	0.10	n.d.	n.d.
SV1 2862	tuff	390	pl, cpx, mt	ms, cc, ep, py, ab	0.071	n.d.	n.d.
M5 1284	lava	230	pl, k-fld, ti-mt	ms, cc, ab, sph	3.87	0.47	17.28
M5 1749	tuff	295	pl, k-fld, ap	ms ,cc ,chl, ab, py	140	-4.08	11.23
M5 2488	reworked	305	k-fld	ms ,cc ,py, qz	0.10	-2.59	10.59
M5 2603	reworked	320	not recognizable crystals		35.3	-3.65	17.41
M5 2604	intrusive	320	pl, k-fld	cc, qz, sid, ep, zr, scap	9.41	-3.55	17.69
M5 2696	tuff	330	cpx, mt	cc, py, qz, sid, ep, scap, sph, amp	17.2	-2.62	16.25
L1 2476	lava	240	k-fld	ab, ser, cc, py	43.4	-1.33	19.37
L1 2638	lava	240	pl, k-fld,ti-mt,ap,bt	ab, ser, cc, py, chl, zeol, fl, pw	67.4	-0.90	16.40
BMS52	syenite		pl, k-fld, cpx, sph	zr, amp, cc	0.40	-3.88	12.37
*M1 1299-1306	lava	295	pl,k-fld,ap,mt,bt	cc, qz, ab, py, ep, ser, ms, chl		-2.4	7.60
*M1 1495-1503	tuffite	320	san,pl,cc,bt,ap	cc, qz , ab, py, ep, ser, chl		-3.1	7.50
†CFDDP 443	tuff	105	k-fld, cpx, bt, mt, pl	alb,cc, py,qz, ms	50-200	-0.24	13.30
†CFDDP 506	tuff	120	k-fld, cpx, bt, mt, pl	alb,cc, py,qz, ms	50-200	-1.83	11.60

Note: Carbon isotopic composition are VS PDB and oxygen VS SMOW. Temperature by De Vivo et al., 1989.k-fld=K-feldspar, mt=magnetite, cpx=clinopyroxene, pl=plagioclase, ap=apatite, ti-mt=Ti-magnetite, bt=biotite, sod=sodalite, ms=sericite, cc=calcite., zeol=zeolite, chl=chlorite, py=pyrite, qz=quartz, amp=amphybole, ep=epidote, sid=siderite, scap=scapolite, sph=sphene, zr=zircon, ab=albite, fl=fluorite, pw=perowskite

* data from Caprarelli et al. (1997)

† data from Mormone et al. (2015). According to most recent measurements (Carlino et al., 2015), obtained in more stabilised conditions, the well CFDDP temperatures are 40°C higher than reported in Mormone et al (2015).

TABLE DR2. SELECTED MICROPROBE ANALYSES OF MINERALS

samples	**L1-2476**	**L1-2476**	**L1-2635**	**L1-2635**	**L1-2635**	**L1-2635**
	albite	pyrite	muscovite	apatite	Ti-mt	k-feld
SiO_2	70.33	0.07	50.73	1.14	0.05	65.95
TiO_2	-	-	0.02	-	7.07	0.02
Al_2O_3	19.39	0.02	29.88	0.02	3.54	18.36
FeO	0.02	65.63	2.56	0.18	82.82	0.03
MnO	0.01	0.05	-	0.13	0.07	-
MgO	-	-	1.51	0.15	0.02	0.01
CaO	0.01	0.01	0.06	53.81	-	0.01
Na_2O	11.68	0.02	0.32	0.22	-	0.59
K_2O	0.04	0.02	9.49	0.02	-	15.15
P_2O_5	-	-	0.01	38.51	-	-
F	-	-	0.69	2.43	-	0.08
Cl	-	-	0.01	0.51	-	-
samples	**L1-2640/43**	**L1-2640/43**	**L1-2640/43**	**L1-2635**	**L1-2635**	**L1-2635**
	biotite	perovskite	fluorite	sphene	gypsium	calcite
SiO_2	48.92	3.09	0.13	30.33	-	-
TiO_2	0.11	48.54	-	33.46	0.03	-
Al_2O_3	30.12	0.77	0.07	4.77	0.06	-
FeO	2.34	1.09	0.03	1.00	0.03	-
MnO	0.00	0.57	-	0.06	0.02	0.33
MgO	1.78	0.26	-	0.00	0.03	-
CaO	0.01	25.05	76.98	28.39	39.87	60.46
Na_2O	0.09	0.05	0.00	0.06	-	0.00
K_2O	9.54	0.01	0.37	0.13	-	0.01
P_2O_5	0.01	0.03	-	0.04	-	-
F	0.65	0.46	44.33	1.63	0.26	0.12
Cl	0.04	0.03	-	0.02	0.01	-
S	-	-	-	-	51.75	-
samples	**L1-2636**	**M5-1749**	**M5-2604**	**M5-2604**	**M5-2604**	**M5-2695**
	chlorite	albite	quartz	siderite	scapolite	pyrite
SiO_2	27.84	66.04	101.96	-	56.72	0.02
TiO_2	0.03	0.04	-	-	0.01	-
Al_2O_3	19.05	20.08	0.01	-	22.09	0.02
FeO	24.14	0.06	0.66	63.56	0.02	47.42
MnO	0.59	0.00	0.00	-	0.02	0.05
MgO	16.04	0.00	0.01	-	0.02	-
CaO	0.13	1.07	0.00	-	7.01	0.02
Na_2O	0.05	6.49	0.01	-	9.51	-
K_2O	0.06	6.46	0.01	-	1.31	-
P_2O_5	-	0.01	0.03	0.05	0.01	-
F	0.34	-0.01	-	0.10	0.01	0.49
Cl	-	-	-	-	3.50	-
S	-	-	-	-	-	45.08

TABLE DR2. CONTINUED

samples	**M5-2695**	**M5-2695**	**SV1 -2222**	**SV1 -2222**	**SV1 -2222**	**SV1 -2222**
	epidote	sphene	quartz	amphibole	chlorite	pyrite
SiO_2	30.21	30.41	95.68	52.41	32.56	0.02
TiO_2	0.33	30.04	-	0.04	0.04	0.01
Al_2O_3	14.97	6.00	1.48	30.78	20.18	0.01
FeO	13.70	1.51	0.05	1.14	5.34	59.99
MnO	0.26	0.08	0.12	0.08	0.22	0.04
MgO	1.05	0.06	0.02	1.67	29.59	-
CaO	12.79	28.73	0.46	12.61	0.06	0.01
Na_2O	-	-	0.30	3.78	0.03	0.01
K_2O	0.01	-	0.26	0.62	0.74	0.01
P_2O_5	0.02	0.01	0.01	0.04	0.00	0.02
F	0.89	2.75	0.53	0.02	0.01	-
Cl	-	-	-	0.16	-	0.27
S	-	0.02	0.03	-	0.01	28.64
samples	**SV1-1714**	**SV1-1418**	**SV1-1418**	**SV1-2130**	**SV1-2130**	**SV1-2130**
	chlorite	calcite	albite	epidote	sericite	chlorite
SiO_2	28.38	0.01	69.24	36.94	36.54	27.77
TiO_2	-	0.01	-	0.20	4.87	-
Al_2O_3	17.93	0.01	20.98	21.53	14.97	16.35
FeO	28.12	0.08	0.04	14.38	13.84	30.73
MnO	2.81	0.46	-	0.36	0.17	1.31
MgO	12.92	-	0.01	0.05	15.98	12.79
CaO	0.08	52.07	0.60	22.35	0.08	0.22
Na_2O	0.04	-	11.25	-	0.32	-
K_2O	-	0.03	0.11	0.14	9.77	0.04
P_2O_5	0.01	-	-	-	-	0.02
F	-	-	-	0.24	-	-
Cl	-	0.36	0.19	-	0.08	0.02
S	-	-	0.04	0.06	0.02	-
samples	**SV1-2130**	**SV1-2130**	**SV1-2863**	**SV1-2863**	**SV1-2863**	**SV1-2863**
	sphene	albite	epidoto	pyrite	ms	albite
SiO_2	30.99	65.93	37.06	0.02	38.30	67.50
TiO_2	27.64	0.08	-	-	2.30	-
Al_2O_3	7.06	20.38	24.52	-	15.47	20.38
FeO	2.10	0.19	11.36	61.17	18.97	0.10
MnO	0.02	0.01	0.21	-	0.28	-
MgO	0.04	0.01	0.04	-	12.85	-
CaO	27.16	1.43	22.88	0.03	-	0.46
Na_2O	0.04	10.63	0.01	0.01	0.16	10.96
K_2O	0.18	0.14	-	0.02	9.85	0.32
P_2O_5	-	0.05	-	-	0.02	0.01
F	2.54	0.08	0.15	0.35	-	0.22
Cl	0.04	0.01	-	0.01	0.02	-

S	-	0.08	-	34.95	0.02	0.01

TABLE DR2. CONTINUED

samples	**BM-S52** mt5	**BM-S52** fluorite	**BM-S52** ilmenite	**BM-S52** horneblende	**BM-S51** scapolite	**BM-S51** pistacite
SiO_2	0.05	0.04	0.01	40.68	59.12	36.60
TiO_2	2.54	-	51.76	2.76	-	0.42
Al_2O_3	0.74	-	0.02	11.05	20.51	5.92
FeO	87.37	0.04	38.88	15.69	0.19	20.10
MnO	2.25	0.02	10.22	0.98	-	4.78
MgO	0.22	-	0.74	10.61	0.03	0.08
CaO	0.04	72.86	0.02	11.48	4.26	29.92
Na_2O	0.02	0.01	0.03	2.42	11.02	0.03
K_2O	-	-	-	2.02	1.57	0.02
P_2O_5	-	-	-	-	0.03	0.01
Cl	0.01	0.02	-	0.10	3.78	-
F	-	43.68	-	1.57	0.01	0.01
S	-	-	-	0.05	-	-

samples	**BM-S51** epidote	**BM-S51** fluorite	**BM-S4** ulvospinel	**BM-S4** sphene	**BM-S4** sphene	**BM-S4** Hauyna
SiO_2	31.02	0.04	0.06	29.58	29.85	32.19
TiO_2	0.63	0.01	2.63	31.24	30.69	0.03
Al_2O_3	13.98	-	0.87	2.96	2.88	27.39
FeO	14.33	0.10	86.21	2.77	2.88	0.21
MnO	0.99	-	2.07	0.20	0.16	-
MgO	0.22	-	0.32	0.17	0.14	-
CaO	13.87	72.15	0.08	27.39	26.62	10.07
Na_2O	-	0.02	0.10	-	0.02	13.86
K_2O	-	0.02	-	-	0.01	3.18
P_2O_5	-	-	-	0.01	0.03	-
Cl	-	0.02	0.01	0.01	0.00	7.15
F	0.14	45.62	0.00	1.57	1.63	0.01
S	-	-	0.25	-	-	4.41

TABLE DR3. MINERAL ZONATION IN CORED SAMPLES AS A FUCTION OF TEMPERATURE

Calcite+Chlorite+illite zone			*Calcite+pyrite+quartz zone*		*Calcite+ epidote zone*		*Alteration zone*
SV1 803	**SV1 1419**	**SV1 1715**	**SV1 2130**	**SV1 2223**	**SV1 2680**	**SV1 2862**	*Mineralogy*
X							*sodalite*
	X						*zeolite*
	X		X			X	*albite*
X	X	X	X		X	X	*illite/sericite*
X	X	X	X	X	X	X	*calcite*
		X	X	X			*chlorite*
X			X	X	X	X	*pyrite*
			X	X			*quartz*
							siderite
			X		X	X	*epidote*
							zircon
							fluorite
							scapolite
							perovskite
			X				*sphene*
				X			*amphibole*
130	**260**	**285**	**300**	**320**	**350**	**390**	**T°C**

Calcite+Chlorite+illite zone			*Calcite+pyrite+quartz zone*		*Calcite+ epidote zone*		*Alteration zone*
L12476	**L12635**	**M5 1284**	**M5 1749**	**M5 2488**	**M5 2604**	**M5 2696**	*Mineralogy*
							sodalite
	X						*zeolite*
X	X	X	X				*albite*
X	X	X	X	X			*illite/sericite*
X	X	X	X	X	X	X	*calcite*
	X						*chlorite*
X			X	X		X	*pyrite*
				X	X	X	*quartz*
					X	X	*siderite*
					X	X	*epidote*
	X				X		*zircon*
	X						*fluorite*
					X	X	*scapolite*
	X						*perovskite*
		X				X	*sphene*
						X	*amphibole*
240	**240**	**230**	**295**	**305**	**320**	**330**	**T°C**

TABLE DR4. CO_2 FLUX FROM CALDERAS

Name	**State**	**feature**	**CO_2-Flux (ton/d)**	**Reference**
Pinatubo	Philippines	lake	884	Perez et al (2011)
Taal	Philippines	lake	739	Perez et al (2011)
Apoyeque	Nicaragua	lake	212	Perez et al (2011)
Apoyo	Nicaragua	lake	539	Perez et al (2011)
Jiloa	Nicaragua	lake	734	Perez et al (2011)
Masaya	Nicaragua	lake	869	Perez et al (2011)
Rotomahana	New Zeland	lake	549	Mazot et al. (2014)
Yellowstone	USA	diffuse soil emission	46000	Werner and Brantley (2003)
Mammoth-LongValley	USA	diffuse soil emission	552	Sorey et al. (1998)
Somma-Vesuvio	Italia	diffuse emission, groundwater	301	Caliro et al. (1995a)
Campi Flegrei	Italia	diffuse soil emission	1500	Chiodini et al. (2001)
Latera	Italia	diffuse soil emission	350	Chiodini et al. (2007)
Colli Albani	Italia	groundwater	500	Chiodini and Frondini (2001)
Furnas	Azzorre	diffuse soil emission	968	Viveiros et al. (2010)
Nisyros	Greece	diffuse soil emission	68	Caliro et al. (2005b)
Teide	Spain	diffuse soil emission	76	Perez et al. (2013)
Rotorua	New Zeland	diffuse soil emission	1000	Werner and Cardellini (2006)
Rotokawa	New Zeland	diffuse soil emission	440	Bloomberg et al. (2014)
El Chichon	Mexico	lake+diffuse soil emission	370	Mazot et al. (2011)

REFERENCES CITED

Agip, 1987, Geologia e geofisica del sistema geotermico dei Campi Flegrei: Unpublished Internal Report, 17 pp.

Bloomberg, S., Werner, C., Rissmann, C., Mazot, A., Horton, T., Gravley, D., Kennedy, B., and Oze, C. , 2014, Soil CO2 emissions as a proxy for heat and mass flow assessment, Taupo Volcanic Zone New Zealand: Geochemistry Geophysics Geosystems, v. 15, p. 4885–4904, doi:10.1002/2014GC005327.

Caliro, S., Chiodini, G., Avino, R., Cardellini, C., Frondini, F. , 2005, Volcanic degassing at Somma-Vesuvio (Italy) inferred by chemical and isotopic signatures of groundwater: Applied Geochemistry, v. 20 (6), p. 1060-1076.

Caliro, S., Chiodini, G., Galluzzo, D., Granieri, D., La Rocca, M., and Ventura G., 2005b, Recent activity of Nisyros volcano (Greece) inferred from structural, geochemical and seismological data: Bulletin of Volcanology, v. 67, p. 358–369, doi:10.1007/s00445-004-0381-7.

Caprarelli, G., Tsutsumi, M., Turi, B., 1997, Chemical and isotopic signature of the basement rocks from the Campi Flegrei geothermal field (Naples, southern Italy): inferences about the origin and evolution of its hydrothermal fluids: Journal of Volcanology and Geothermal Research, v. 76, p. 63–82.

Carlino, S., Somma, R., Troise, C., and De Natale, G., 2015, Campi Flegrei Deep Drilling Project: an overview of main results and implications on caldera dynamic. AGU Joint Assembly, 3-7-May 2015, Abstract, p. 560,Canada.

Chiodini, G., Baldini, A., Barberi, F. , Carapezza, M. L., Cardellini, C., Frondini, F., Granieri, D. , and Ranaldi, M., 2007, Carbon dioxide degassing at Latera caldera (Italy): Evidence of geothermal reservoir and evaluation of its potential energy: Journal Geophysical Research, v. 112, B12204, doi:10.1029/2006JB004896.

Chiodini, G., Frondini, F., 2001, Carbon dioxide degassing from the Albani Hills volcanic region, Central Italy: Chemical Geology, v. 177, p. 67–83.

Chiodini, G., Frondini, F., Cardellini, C., Granieri, D., Marini, L., Ventura, G., 2001, CO_2 degassing and energy release at Solfatara volcano, Campi Flegrei, Italy: Journal of Geophysical Research B, Solid Earth, v. 106 (B8), p. 16213-16221.Mazot, A., Rouwet, D., Taran, Y., Inguaggiato, S., Varley, N., 2011, CO_2 and He degassing at El Chichón volcano, Chiapas, Mexico: gas flux, origin and relationship with local and regional tectonics: In Inguaggiato, S., Shinohara, H., and Fischer, T. (eds) Geochemistry of volcanic fluids: a special issue in honor of Yuri A. Taran: Bulletin Volcanology, v. 73(4), p. 423–442.

Mazot, A., Schwander, F., Christenson, B., de Ronde, C. E.J., Inguaggiato, S., Scott, B., Graham, D., Britten, K., 2014, CO_2 discharge from the bottom of volcanic Lake Rotomahana, New Zealand: G3 v. 15, 3. doi: 10.1002/2013GC004945.

Mormone, A., Troise, C., Piochi, M., Balassone, G., Joachimski, M., De Natale, G., 2015, Mineralogical, geochemical and isotopic features of tuffs fromthe CFDDP drill hole: Hydrothermal activity in the eastern side of the Campi Flegrei volcano (southern Italy): Journal Volcanology Geothermal Research http://dx.doi.org/10.1016/j.jvolgeores.2014.12.003.

Pérez, N.M., Hernández, P.A., Padilla, G., Nolasco, D., Barrancos, J,. Melián,, G., Padrón, E., Dionis, S., Calvo, D., Rodríguez, F., Notsu, K., Mori, T.,Kusakabe, M., Arpa, M.C., Reniva, P., Ibarra ,M ., 2011, Global CO_2 emission from volcanic lakes: Geology, v. 39(3), p. 235–238, doi:10.1130/G31586.1.

Perez, N.M., Hernandez, P.A., Padron, E., Melin, G., Nolasco, D., Barrancos, J., Padilla, G., Calvo, D., Rodriguez, F., Dionis, S., Chiodini, G. , 2013, An increasing trend of diffuse CO_2 emission from Teide volcano (Tenerife, Canary Islands): Geochemical evidence of magma degassing episodes: Journal of the Geological Society, v. 170 (4), p. 585-592.

Rosi, M., & Sbrana, A., 1987, Phlegrean Fields. CNR, Quaderni Ricerca Scientifica 114, 175 pp.

Sinclair, A.J., 1974, Selection of threshold values in geochemical data using probability graphs: Journal of Geochemical Exploration, v.3, p. 129 -149.

Sorey, M.L., Evans, W.C., Kennedy, B.M., Farrar, C.D., Hainsworth, L.J., Hausback, B., 1998, Carbon dioxide and helium emissions from a reservoir of magmatic gas beneath Mammoth Mountain, California: Journal Geophysical Research, v. 103, p. 15303-15323.

Viveiros, F., Cardellini, C., Ferreira, T., Caliro, S., Chiodini, G. , and Silva C., 2010, Soil CO_2 emissions at Furnas volcano, São Miguel Island, Azores archipelago: Volcano monitoring perspectives, geomorphologic studies, and land use planning application: Journal Geophysical Research, v. 115, B12208, doi:10.1029/2010JB007555.

Werner, C., and Brantley, S., 2003, CO_2 emissions from the Yellowstone volcanic system, Geochemistry Geophysics Geosystems, v. 4, 1061, doi:10.1029/2002GC000473.

Werner, C., Cardellini, C., 2006, Comparison of carbon dioxide emissions with fluid upflow, chemistry, and geologic structures at the Rotorua geothermal system, New Zealand: Geothermics, v. 35 (3), p. 221-238.